

Contribution of the $2p-1h$ Multiple Scattering Correlation to the Spectra of ^{17}O and ^{15}O

Wu Shishu, Yang Shande and Li Yuncui
(Department of Physics, Jilin University, Chang Chun)

Using the method of Green's function and partial summation of multiple scattering, we have investigated in various approximations the contribution of $2p-1h$ multiple scattering correlation to the low energy spectrum of ^{17}O and ^{15}O , respectively. In our calculation, the nuclear force employed is the Paris potential and the energy dependence of \underline{G} matrices has been taken into account rigorously. The numerical results agree with the experimental data reasonably well.

1. INTRODUCTION

We shall only consider the two-body interaction. In the non-relativistic approximation the nuclear Hamiltonian may be written as

$$H = H_0 + H_1 \quad (1)$$

$$H_0 = T + U = \sum_{i=1}^N (t_i + u_i) = \sum_{i=1}^N h_i \quad (2)$$

$$H_1 = V - U = \sum_{i>j=1}^N v_{ij} - \sum_{i=1}^N u_i. \quad (3)$$

Received on June 3, 1987.

Where T is the total kinetic energy operator, V the interaction potential, H_1 the residual interaction, N the total number of nucleons and u the single particle (sp) potential introduced for the facility of calculation.

Our aim is to find an approximate method which is adequate for the calculation of the mass operator (MO). In this paper we would like to investigate the contribution of the $2p-1h$ multiple scattering correlation by means of the method of Green's functions[1] (MGF) and through the calculation of the sp and sh (single hole) spectrum. According to MGF, there are two ways to calculate the sp (sh) spectrum. One is to make use of the sp Schrödinger equation with u defined in terms of MO. It has been shown that this MO potential is an optimal choice according to the principle of maximum cancellation and the principle of maximum overlap[2]. However, the equation has to be solved self-consistently. The result of our calculation will be reported in a succeeding paper. Here we shall follow the other method which is simpler and consists of solving an eigenvalue equation derived from the sp Green function. The contribution of the $2p-1h$ vertex and its various higher order corrections to the sp spectrum of ^{17}O has already been considered by Kuo, Bando and many others[3--6]. To compare with their results, we have used a different method and put our emphasis on an analysis of the effects caused by different sets of diagrams and various approximations. In order to gain some insight into the importance of the contribution of the $2p-1h$ correlation to the hole states, we have further calculated the sh spectrum of ^{15}O .

We shall describe the method of calculation in Sect.2. In Sect.3 the results will be presented and discussed. A brief summary is given in Sect.4.

2. METHOD OF GREEN'S FUNCTIONS AND $2p-1h$ MULTIPLE SCATTERING CORRELATION

In the second quantization representation, Eqs.(2) and (3) may be rewritten as

$$H_0 = \sum_{\alpha\beta} h_{\alpha\beta} \xi_{\alpha}^{\dagger} \xi_{\beta} = \sum_{\alpha\beta} (t_{\alpha\beta} + u_{\alpha\beta}) \xi_{\alpha}^{\dagger} \xi_{\beta}, \quad (4)$$

$$H_1 = \frac{1}{4} \sum_{\alpha\beta\gamma\delta} v_{\alpha\beta\gamma\delta} \xi_{\alpha}^{\dagger} \xi_{\beta}^{\dagger} \xi_{\gamma} \xi_{\delta} - \sum_{\alpha\beta} u_{\alpha\beta} \xi_{\alpha}^{\dagger} \xi_{\beta}, \quad (5)$$

where $\xi_{\alpha}^{\dagger}(\xi_{\alpha})$ is the creation (annihilation) operator for the sp state $|\alpha\rangle$ and $v_{\alpha\beta\gamma\delta}$ the antisymmetrized matrix element of the two-body interaction. According to the theory of Green's functions, the sp(sh) spectrum can be obtained from the following eigenvalue equation:

$$\sum_{\gamma} [(\epsilon_{\alpha} - \mathcal{E}_{\gamma}^{\pm}) \delta_{\alpha\gamma} + M_{\alpha\gamma}(\mathcal{E}_{\gamma}^{\pm}) - u_{\alpha\gamma}] C_{\gamma}^{\pm} = 0, \quad (6)$$

where ϵ_{α} satisfies

$$h|\alpha\rangle = \epsilon_{\alpha}|\alpha\rangle, \quad (7)$$

$$\mathcal{E}_{\gamma}^{\pm} = \pm [E_n(A \pm 1) - E_0(A)], \quad (8)$$

$$C_{\gamma}^{\pm} = \begin{cases} \langle \psi_0 | \xi_{\gamma} | \psi_n(A+1) \rangle \\ \langle \psi_n(A-1) | \xi_{\gamma} | \psi_0 \rangle \end{cases} \quad (9)$$

$|\psi_0\rangle$ is the rigorous ground state wave-function of a closed-shell nucleus with the mass number A , $E_0(A)$ its corresponding energy, while $|\psi_n(A \pm 1)\rangle$ and $E_n(A \pm 1)$ denote the rigorous eigenfunction and energy eigenvalue of nucleus with the mass number $A \pm 1$ respectively. According to Eq.(8), \mathcal{E}_n^\pm are the eigenvalues we want to find. Though $M_{\alpha\tau}(\mathcal{E}_n^\pm)$ depends on \mathcal{E}_n^\pm , Eq.(6) can be solved easily by a self-consistent procedure. Clearly our results will depend on what approximation we make for the calculation of the mass operator $M_\alpha\gamma$, which is an infinite sum of irreducible vertices. Usually $M_\alpha\gamma$ is calculated by the method of partial summation. One of our purposes is to gain more insight into the importance of the contribution from different classes of Feynman diagrams through an actual calculation.

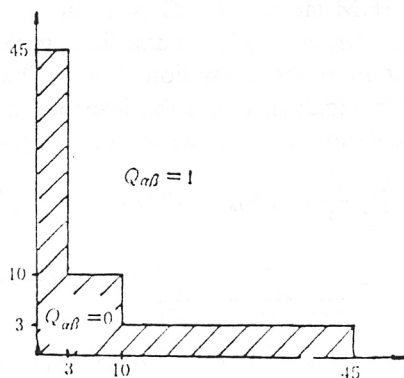


FIG.1 Model space for the calculation of G -matrix.

$$(n_1, n_2, n_3) = (3, 10, 45)$$

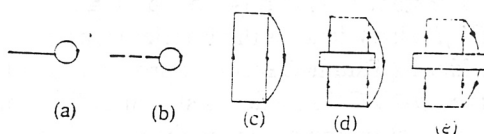


FIG.2 Diagrams considered in the calculation of $M_{\alpha\beta}$. "—" and "----" indicate that the model spaces for the calculation of G -matrices are $(n_1, n_2, n_3) = (3, 10, 45)$ and $(3, 3, 45)$, respectively.

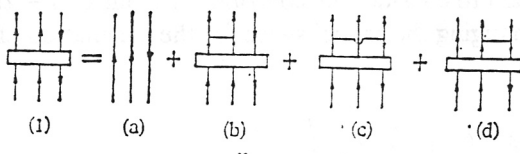


FIG.3 Integral equation for the $2p-1h$ GF in TDA.

For simplicity, u will be taken as the harmonic oscillator potential, namely

$$u = \frac{1}{2} m\Omega^2 r^2 + C \quad (10)$$

where Ω is the oscillator frequency and C a zero-point energy constant. In our calculation $M_{\alpha\gamma}$ is expanded in terms of the G -matrices which, as is well known, are defined as

$$G_B(\omega) = V + V \frac{Q}{\omega - H_0(2)} G_B(\omega), \quad (11)$$

where Q denotes the Pauli exclusion Operator, ω an energy variable and $H_0(2)$ the unperturbed 2-particle Hamiltonian determined by u . We have used the G -matrices calculated from the Paris potential[8] according to the BHM method[9]. $\hbar\Omega$ is taken to be 16 MeV and the model space is chosen as shown in Fig.1, where (n_1, n_2, n_3) is the notation employed by Kuo[3].

Fig.2(a) gives the lowest order approximation to $M_{\alpha\beta}$. The $2p$ - $1h$ irreducible vertex which we have considered is presented in Fig.2(e), where the insertion as Fig.3(1) denotes a $2p$ - $1h$ Green function. The formulae of calculation for Fig.2(a) and (e) are given by

$$\text{Fig. (a)} \equiv M_{\alpha\beta}^{(1)}(\omega) = \sum_{\Gamma\hbar} \frac{\hat{\Gamma}}{\hat{\alpha}} \Delta_{\alpha\hbar} \Delta_{\beta\hbar} \langle \alpha\hbar\Gamma | G_B(\omega + \varepsilon_h) | \beta\hbar \rangle \delta_{i_\alpha i_\beta}, \quad (12)$$

$$\begin{aligned} \text{Fig. (e)} \equiv M_{\alpha\beta}^{2p1h}(\omega) = & - \sum_{m \leq n} \sum_{r \leq s} \sum_{k l} \sum_{\Gamma_1 \Gamma_2} (-1)^{\alpha+\beta+k+l+\Gamma_1+\Gamma_2} \cdot \frac{\hat{\Gamma}_1 \hat{\Gamma}_2}{\hat{\alpha} \hat{\beta}} \Delta_{\alpha k} \Delta_{\beta l} \\ & \times \langle \alpha k \Gamma_1 | G_B(\omega + \varepsilon_k) | m n \Gamma_1 \rangle G(m n(\Gamma_1) k[\alpha], r s(\Gamma_2) l[\alpha]; \omega) \\ & \times \langle r s \Gamma_2 | G_B(\omega + \varepsilon_l) | \beta l \Gamma_2 \rangle \delta_{i_\alpha i_\beta} \end{aligned} \quad (13)$$

where $\langle \alpha\beta\Gamma | G_B(\omega) | \gamma\delta\Gamma \rangle$ is an anti-symmetrized and normalized G -matrix element, $\Delta_{\alpha\beta} \equiv \sqrt{1 + \delta_{\alpha\beta}}$ and α a shorthand for a complete set of sp quantum numbers $(\alpha\alpha)$, while α in the round bracket and Γ stand for the angular momentum as well as the isospin quantum numbers of a sp and a two-particle system respectively; for instance, $(-1)^\alpha \equiv (-1)^{\alpha + \alpha'}$, $\Gamma \equiv JT$, $\hat{\Gamma} \equiv \sqrt{(2J+1)(2T+1)}$ etc.. In Eq.(13) $G(mn(\Gamma_1)k[\alpha], rs(\Gamma_2)l[\alpha]; \omega)$ denotes the Fourier transform of the $2p$ - $1h$ Green function (GF). Here we shall only consider its Tamm-Dancoff approximation (TDA). In this approximation the integral equation which the $2p$ - $1h$ GF satisfies is shown in Fig.3 and its analytic expression is given in the appendix. In our calculation the exchange diagrams in the intermediate states and the energy dependence of G matrices have been fully taken into account.

From Figs.2(e) and 3 it can be easily seen that Fig.2(e) reduces to 2(c) if in Fig.3 only diagram (a), i.e. the zeroth order approximation to the $2p$ - $1h$ GF, is considered, while Fig.2(e) reduces to 2(d) if both diagrams (a) and (b) in Fig.3 are taken into account. Obviously, Fig.2(c) is an approximation of 2(d). When we only want to consider the contribution from 2(a) + 2(d), we note that this can also be achieved by simply changing the model space for the calculation of G -matrices

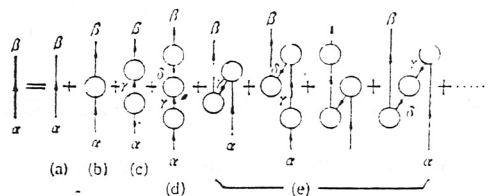


FIG.4 Series expansion of $G_{\alpha\beta}(\omega)$ in terms of $v_{\alpha\gamma}^{eff}(\omega) = u_{\alpha\gamma} - M_{\alpha\gamma}(\omega)$.

form $(n_1, n_2, n_3) = (3, 10, 45)$ to $(3, 3, 45)$. Then, the lowest order approximation to $M_{\alpha\beta}$ becomes Fig.2(b) instead of 2(a) and we clearly have $2(b) = 2(a) + 2(d)$. However, if we want to further consider Fig.2(e), we must choose $(n_1, n_2, n_3) = (3, 10, 45)$, otherwise redundant terms will occur in the integral equation shown in Fig.3. Fig.4 shows the series expansion of $G_{\alpha\beta}(\omega)$ in terms of $v_{\alpha\gamma}^{eff} \equiv u_{\alpha\gamma} - M_{\alpha\gamma}(\omega)$, which is represented symbolically by "o" in the figure. Clearly, if we truncate Eq.(6) to a set of n_i equations, it implies that in this approximation γ, δ , etc. in Fig.4 only run over n_i intermediate states. For instance, if we choose $n_i = 1$, this means that we only allow $\gamma = \delta = \dots = \alpha = \beta$ and a vast number of diagrams in Fig.4 are neglected except those with $v_{\alpha\gamma}^{eff} = \delta_{\alpha\gamma} v_{\alpha}^{eff}$. For finite nuclei this may be a poor approximation, since $v_{\alpha\gamma}^{eff}$ is not diagonal. Thus, how to choose an appropriate n_i is worth studying.

3. RESULTS AND DISCUSSION

In order to compare and assess the importance of the contributions from different classes of Feynman diagrams, we have treated $M_{\alpha\beta}$ in 4 different approximations. The numerical results obtained from Eq.(6) are listed in Table 1, where the Latin letters a--e refer to the diagrams in Fig.2. From Table 1 we can easily get the additional contribution[i] due to the consideration of diagram (i) besides (a), namely $[i] = (a + i) - a$ ($i = c, d$, or e). Their values are listed in Table 2. Note that [i] includes the interference terms between the irreducible vertex (i) and (a). Thus, if [i] is small, the addition of (i) is unnecessary. One can see further that (d)-(c) gives the additional contribution of the pp scattering correlation in the $1s-0d$ and $1p-0f$ shell (as illustrated in Fig.1, scattering to states above the $1p-0f$ shell has already been taken into account by the G -matrices), while (e)-(d) gives the additional contribution from the ph scattering. They will hereafter be referred to as the pp SC and ph SC, respectively and their values are presented in the last two rows of Table 2. It can be seen that the contributions from (d) and (e) are almost the same. This shows that ph SC is small and

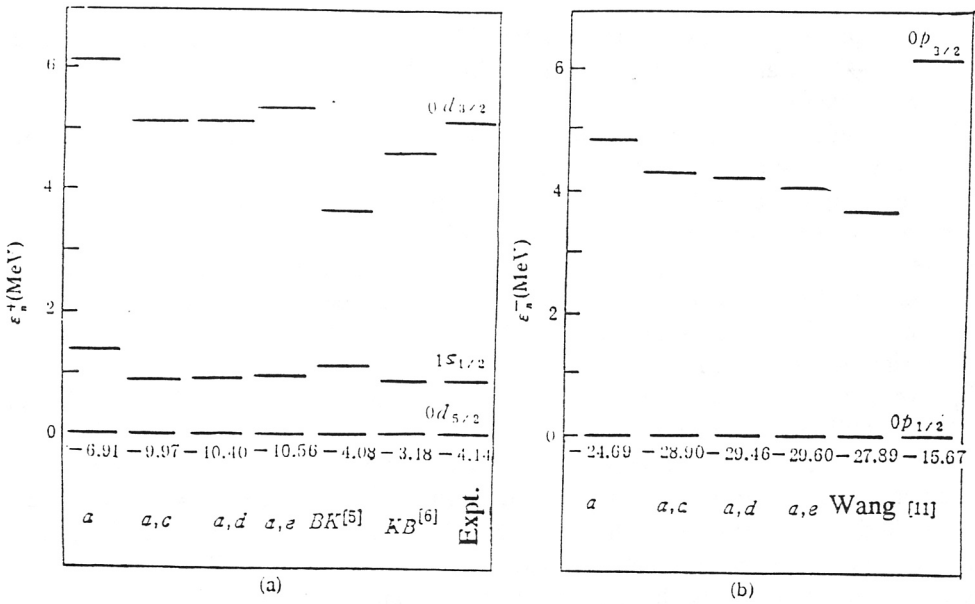


FIG.5 (a) Spectrum of ^{17}O ; (b) Spectrum of ^{15}O .

TABLE 1 Calculated Spectrum of ^{15}O and ^{17}O with $C = -58 \text{ MeV}$, $\hbar\Omega = 16 \text{ MeV}$ (Unit: MeV)

Diagram \ State	$0s_{1/2}$	$0p_{3/2}$	$0p_{1/2}$	$0d_{3/2}$	$1s_{1/2}$	$0d_{5/2}$
a	-54.13	-29.46	-24.69	-6.91	-5.48	-0.85
a,c	-56.73	-33.06	-28.90	-9.97	-9.09	-4.87
a,d	-57.25	-33.55	-29.46	-10.40	-9.51	-5.28
a,e	-57.31	-33.58	-29.60	-10.56	-9.68	-5.32
Expt.	-46 ± 8	-21.85	-15.67	-4.14	-3.27	0.944

TABLE 2 Contribution of Different Diagrams to the Spectrum of ^{15}O and ^{17}O (Unit: MeV)

Contribution \ State	$0s_{1/2}$	$0p_{3/2}$	$0p_{1/2}$	$0d_{3/2}$	$1s_{1/2}$	$0d_{5/2}$
Diagram						
[c]	-2.60	-3.60	-4.21	-3.06	-3.61	-4.02
[d]	-3.12	-4.09	-4.77	-3.49	-4.03	-4.43
[e]	-3.18	-4.12	-4.91	-3.63	-4.20	-4.47
[d]-[c]=[pp]	-0.52	-0.49	-0.56	-0.43	-0.42	-0.41
[e]-[d]=[ph]	-0.06	-0.03	-0.14	-0.16	-0.17	-0.04

comparatively unimportant, though it has some noticeable effect on the energy difference between the lower spectra of both ^{15}O and ^{17}O obtained from (c) by 0.5 MeV. From the results listed in Tables 1 and 2 we may conclude that

(i) it does not suffice to consider Diagram 2(a) only, because according to Table 2, Diagram 2(d) or (e) may lower its result by more than 3 MeV;

(ii) Diagram 2(b) = 2(a) + 2(d) is a quite good approximation of 2(a) + 2(e).

In the calculation we have chosen $C = -58 \text{ MeV}$ in Eq.(10) so as to match the average energy of the $0p$ and $1s-0d$ shell with the experimental value. The dependence of our results on C will further be discussed at the end of this section. We have not considered the correction due to the spurious center of mass (c.m.) motion since it has been found in Ref.[10] that the effect of this correction is not significant when $M_{\alpha\beta}$ is calculated by Fig.2(b).

In Fig.5 we have plotted our results and those calculated previously by BK[5], KB[6] and Wang et al.[11]. Ref.[5] has considered Figs.2(a) and 2(e), while Ref.[6] has, in addition, taken account of the corrections due to the one-body G -matrix vertices and the c.m. motion. In their calculation they have used the Reid potential and taken $\hbar\Omega = 14 \text{ MeV}$ and $C = -54 \text{ MeV}$. Even though their method is different from ours, we note that their calculation tacitly involves an approximation which corresponds to the one we used when we truncate Eq.(6) to $n_i = 1$. Wang et al. have used the same method as we do. They have done a comparison of the sp and sh spectrum calculated by the Hamada-Johnston, the soft Reid and the Paris potential with $C = 0, -15, -32$ and -49 MeV . However, they have only considered Fig.2(b). Since their Paris potential result is almost the same as that given in the column (a + d), we have only plotted their Reid potential result with $C = -49 \text{ MeV}$ for comparison.

From Fig.5 it can be seen that for ^{17}O Diagram 2(a) gives a too large level distance (LD). It improves significantly and agrees well with the experimental value, if Diagram 2(c), (d) or (e) is

further taken into account, though the energy value of level $0d$ ($E[d_{5/2}]$) becomes lower and worse. $E[d_{5/2}]$ obtained by BK and KB is better than ours, however their result for LD is poorer, even though noticeable improvement has been gained by KB through additional consideration of corrections mentioned above. Since $\epsilon_{\alpha}\delta_{\alpha\beta} - u_{\alpha\beta} = t_{\alpha\beta}$, it is seen that the result of Eq.(6) should be independent of Ω and C if it is solved rigorously. In case of an approximate calculation, Ω and C may be regarded as effective parameters. Our result confirms what has been found by Refs.[10] and [11] for LD, namely

- (i) $\hbar\Omega = 16$ MeV is a better choice than $\hbar\Omega = 14$ MeV for nuclei in the neighborhood of ^{16}O ;
- (ii) the Paris potential is more preferable than the Reid potential, though the former makes $E[d_{5/2}]$ lower.
- (iii) though C has a clear effect on $E[d_{5/2}]$, LD is almost independent of C . The latter is indeed a very desirable result.

In Fig.6 we have plotted our calculated result for the dependence of the sp spectrum on C . The dashed line indicates the experimental value. If we choose $C = -16$ MeV, we get $E[d_{5/2}] = -4.08$ MeV, $E[s_{1/2}] = -3.24$ MeV and $E[d_{3/2}] = 1.17$ MeV. This is a very good result for both LD and $E[d_{5/2}]$. However, if we want to take account of the sp and sh spectrum at the same time, the choice of $C = -58$ MeV seems more appropriate. Obviously, this is something which should be studied further and the good agreement with experiment through adjustment of C may not mean much.

TABLE 3 Convergence Behavior of the Truncation Approximation for the ^{17}O Spectrum ($C = 0$; unit: MeV)

State	$0d_{5/2}$		$1s_{1/2}$		$0d_{3/2}$	
N_t	1	4	1	5	1	4
Energy	-1.60	-2.41	0.07	-1.73	4.60	2.72

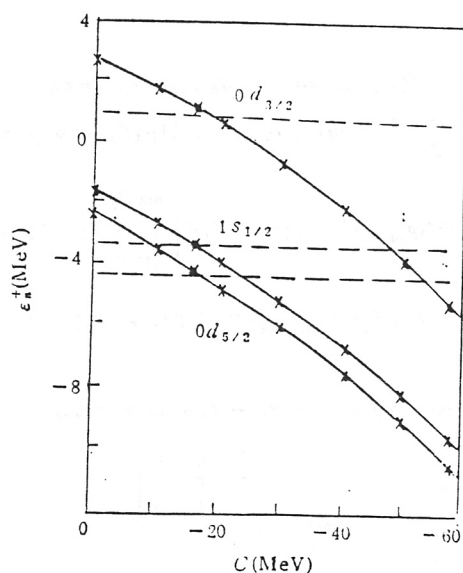


FIG.6 Dependence of the spectrum of ^{17}O on C .

Fig.5(b) shows the calculated sh spectrum of ^{15}O . We see that the level splitting of the p -state calculated either by us or by Ref.[11] is too small, though ours is somewhat better, because we have used the Paris potential. It is rather bothering that the consideration of additional diagrams

2(c), (d) and (e) makes the result even worse. This clearly shows that some important effects have not yet been taken into account.

Ref.[10] has studied the convergence behavior of the truncation approximation for the solution of Eq.(6). It is found that the result for hole states converges quickly, but for particle states one has to choose $nt \geq 4$. We have restudied the problem. The result of our calculation for the Paris potential is given in Table 3. It is seen that $nt = 1$ only gives a poor result.

4. SUMMARY

We have calculated the contribution of the $2p$ - $1h$ multiple scattering to the sp and sh spectrum in the region and Diagram 2(b) is a good approximation to $2(a) + 2(e)$. Since 2(b) is much easier to handle, this will simplify the calculation a great deal. However, our result for the p -level splitting and $E[d_{5/2}]$ is still too poor. It has been shown [3,4,13] that the $3p2h$ diagram, which will be referred to by us from the view-point of MO as the $2h$ - $1p$ (irreducible) vertex, may give each sp level of ^{17}O a uniform repulsion of about 1 MeV. Clearly, this vertex may be even more important for the hole states. We have studied the additional contribution of the $2h$ - $1p$ multiple scattering. Our result will be reported in a succeeding paper. As we have mentioned in the previous section, our result depends on Ω and C . It is not difficult to see that this undesirable aspect can be avoided easily by the method of the MO potential. What the latter may achieve is also being studied.

ACKNOWLEDGEMENT

We are very grateful to Profs. X. G. Jing and K. X. Wang for their help in the numerical calculation.

APPENDIX

$$\begin{aligned}
 G_{\text{TDA}}(mn(\Gamma_1)k[\Gamma], rs(\Gamma_2)l[\Gamma], \omega) = & -\delta_{mr}\delta_{kt}\delta_{st}\delta_{\Gamma_1\Gamma_2}g^0(mnk;\omega) \\
 & + g^0(mnk;\omega) \sum_{p \leq q} \sum_{j\Gamma_3} \left\{ \langle mn\Gamma_3 | G_B(\omega + \varepsilon_k) | pq\Gamma_3 \rangle \delta_{jk}\delta_{\Gamma_3\Gamma_1} + [1 - (-1)^{m+n-\Gamma_1}P_{mn}] \right. \\
 & \times [1 - (-1)^{p+q-\Gamma_3}P_{pq}] \sum_{\Gamma_4} (-1)^{n+k+j+\Gamma_4+\Gamma} \left\{ \begin{matrix} mn\Gamma_1 \\ \Gamma_4 P k \\ j\Gamma_3\Gamma \end{matrix} \right\} \langle j\Gamma_4 | G_B(\omega + \varepsilon_k + \varepsilon_j - \varepsilon_s) | kP\Gamma_4 \rangle \\
 & \left. \times \delta_{qs}\Delta_{mn}^{-1}\Delta_{pq}^{-1}\hat{\Gamma}_1 \cdot \hat{\Gamma}_3 \cdot \hat{\Gamma}_4^z \right\} G_{\text{TDA}}(pq(\Gamma_3)j[\Gamma], rs(\Gamma_2)l[\Gamma]; \omega), \quad (1)
 \end{aligned}$$

where

$$\begin{aligned}
 g^0(mnk;\omega) = & \{\omega - \varepsilon_m - \varepsilon_s + \varepsilon_k + i\eta\}_{\eta \rightarrow 0^+}, \quad (2) \\
 \left\{ \begin{matrix} mn\Gamma_1 \\ \Gamma_4 P k \\ j\Gamma_3\Gamma \end{matrix} \right\} = & \left\{ \begin{matrix} jmi_nJ_1 \\ J_4 I_p I_k \\ jJ_3J \end{matrix} \right\} \cdot \left\{ \begin{matrix} \frac{1}{2} & \frac{1}{2} & T_1 \\ T_4 & \frac{1}{2} & \frac{1}{2} \\ \frac{1}{2} & T_3 & T \end{matrix} \right\}, \quad (3)
 \end{aligned}$$

and P_{mn} denotes the exchange operator which exchanges m with n .

REFERENCES

- [1] S. S. Wu and Y. J. Yao, *Chinese Journal of Nuclear Physics* **2**(1980), 193.
- [2] S. S. Wu Proceedinge of the International Summer School on nucleon-nucleon interaction and nuclear munybody problems ed. S. S. Wu and T. T. S. Kuo (world. Scientific 1983)321.
- [3] T. T. S. Kuo et al., *Nucl. Phys.* **85**(1966), 40.
- [4] K. C. Tam et al., *Nucl. Phys.* **A361**(1981), 412.
- [5] H. Bando et al., *Nucl. Phys.* **A273**(1976), 95.
- [6] E. M. Krenciglowa et al., *Nucl. Phys.* **A294**(1978), 191.
- [7] K. A. Brueckner et al., *Phys. Rev.* **110**(1958), 431.
- [8] R. Vinh Mau, In *Mesons in Nuclei*. P151 edited by M. Rho and D. Wilkinson (Morth-Holland Publishing Co. Amsterdam 1979).
- [9] B. R. Barrett et al., *Phys. Rev.* **C3**(1971), 1137.
- [10] S. D. Yang et al., *Physica Energiae Fortis et Physica Nuclearis* **6**(1982), 484.
- [11] K. X. Wang et al., *Physica Energiae Fortis et Physica Nuclearis* **6**(1982), 525.
- [12] R. V. Reid, *Ann of Phys.* **50**(1968), 411.
- [13] E. M. Krenciglowa et al., *Nucl. Phys.* **A322**(1979), 145.